

Chapter 2

Study of the Dynamics of 5CB Thin Layer Placed on the Fullerene Wall: Computer Simulations

Przemysław Raczyński and Zygmunt Gburski

2.1 Introduction

The properties of liquid crystals are still not fully explored, and they are intensively studied, also using MD technique [1–8]. These studies are motivated by the search for the materials suitable for the new generation of displays, and our research follows that line. In view of this, the combination of liquid crystals with a specific carbon nanostructure is the subject of our studies. The molecule 5CB, with the chemical formula $C_{18}H_{19}N$, was first synthesized from the series of n-cyanobiphenyls, an important group of mesogens. The aim of our research was to find a mesogen with the specific intention of using it in liquid crystal displays (LCD).

Nanostructures, such as graphene, nanotubes, or fullerenes, exhibit interesting physical properties [9–17], and they are still intensively studied. C60, called buckminsterfullerene, is the most famous and very carefully examined. It is the most common naturally occurring molecule of fullerenes' family, which can be found, for example, in soot.

In this work we describe the properties of the molecular system consisted of C60 and 5CB. Mesogen molecules were placed on the surface composed of two fullerene layers. This system was studied for a wide range of temperatures, from 240 to 390 K, for a thorough examination of the behavior of 5CB. The properties of mesogens placed on the surface consisted of fullerenes C60 are interesting for scientific reasons and potential applications.

P. Raczyński (✉) • Z. Gburski

Institute of Physics, University of Silesia, Uniwersytecka 4, 40-007 Katowice, Poland

e-mail: przemyslaw.raczyński@us.edu.pl

© Springer International Publishing Switzerland 2016

O. Fesenko, L. Yatsenko (eds.), *Nanophysics, Nanophotonics, Surface Studies, and Applications*, Springer Proceedings in Physics 183,

DOI 10.1007/978-3-319-30737-4_2

2.2 Simulation Details

All simulations were performed using NAMD 2.8 simulation code [18] and visualized in VMD [19].

The model of 5CB mesogen molecule has been adopted from the CHARMM-type united atom potential developed by Tiberio and co-workers [20]. C60 molecule has been modeled using all-atom potential described elsewhere [21, 22].

Interactions between the mesogens have been described using electrostatics and van der Waals forces modeled with coulombic and Lennard–Jones 12-6 potential, respectively. Cutoff was equal to 12 Å. Interactions between C60 and 5CB molecules have been described with van der Waals interactions modeled with Lennard–Jones 12-6 potential. Periodic boundary conditions were applied on x - and y -axes to treat fullerene surface as an infinite. Equations of motion were integrated using Brunger–Brooks–Karplus (BBK) scheme, implemented in NAMD, with the time step of integration equal to 0.5 fs.

All simulations were performed in NVT ensemble, for temperatures $T = 240, 270, 300, 330, 360$, and 390 K. Between successive temperatures, the system was slowly heated and, next, equilibrated for 1 ns. After that, the simulation runs when the data were collected were performed for 10 ns. To check the reproducibility, all runs were repeated.

We prepared “C60 surface” consisted of the two layers. Fullerenes in the layer adjacent to the mesogen molecules were not fixed. In the second C60 layer, two of the fullerene atoms were fixed.

2.3 Results

Figure 2.1 shows the snapshot of the instantaneous configuration of the studied system after all performed simulations. Some of the 5CB molecules tried to penetrate C60 surface by immersing themselves between fullerene molecules. This process is slight in the low temperatures studied, and it proceeds with the heating of the cluster because mesogen molecules become more mobile.

The process of increasing dynamics of 5CB molecules with the heating of the cluster can be observed in the mean square displacement $\langle |\Delta \vec{r}(t)|^2 \rangle$ plots of the center of mass of a single molecule. It can be also confirmed by evolution of the diffusion coefficient D : $\langle |\Delta \vec{r}(t)|^2 \rangle \approx 6Dt$.

Figure 2.2 shows the $\langle |\Delta \vec{r}(t)|^2 \rangle$ plots of the center of mass of 5CB. For the clarity only first 5 ns for the three different temperatures is shown. Table 2.1 shows obtained values of the diffusion coefficient D .

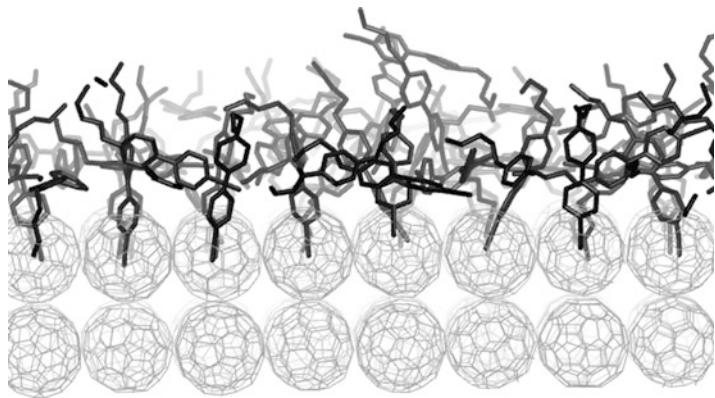


Fig. 2.1 The snapshot of the final configuration of the studied system

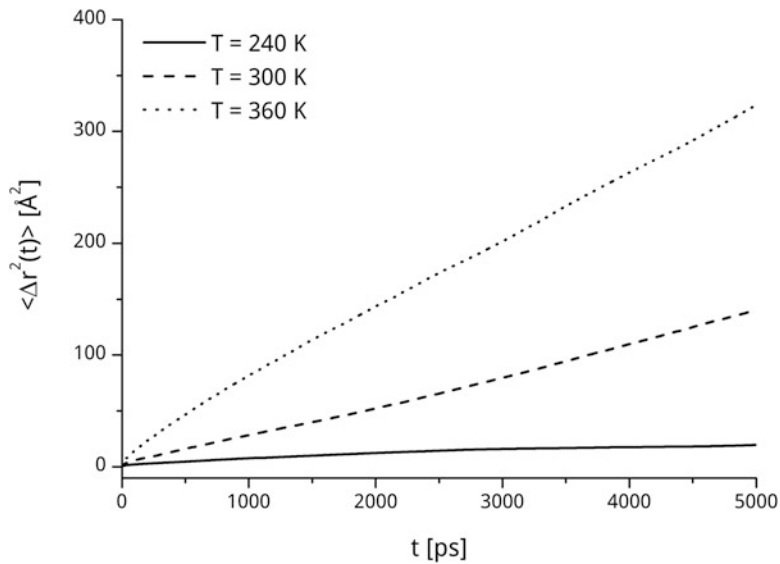


Fig. 2.2 The mean square displacement of the center of mass of 5CB molecule

Table 2.1 Obtained values of the diffusion coefficient D

T (K)	D ($\text{\AA}^2/\text{ps}$)
240	0.002
270	0.003
300	0.007
330	0.011
360	0.021
390	0.033

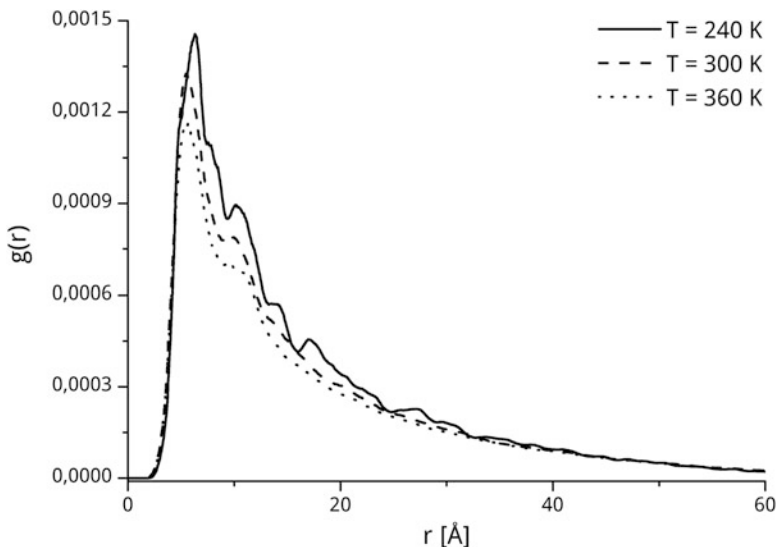


Fig. 2.3 The radial distribution function of the center of mass of 5CB molecule

The $\langle |\Delta \vec{r}(t)|^2 \rangle$ plots and related values of D show that the 5CB molecules became more mobile with an increasing of the temperature of the system.

The plot of $\langle |\Delta \vec{r}(t)|^2 \rangle$ for the lowest temperature studied is typical for the solid state. The shape of $g(r)$ for this temperature, shown in Fig. 2.3, confirms that 5CB molecules are in the solid state, because first and next peaks are sharp and clearly visible. The first peak of $g(r)$ function corresponds to the nearest neighbor distance, and next peaks reflect a distance to the further neighbors. Contrary to $g(r)$ at the lowest temperature, the next peaks at higher temperatures studied are not so much visible. Only the first and second peaks can be observed for the higher temperatures. The differences in $g(r)$ plots between the lowest and the highest temperatures indicate an occurrence of the phase transition.

To confirm this conclusion, the evolution of the Lindemann index δ_L is shown in Fig. 2.4, where the “jump” between 270 and 300 K is observed. This jump indicates the phase transition between these temperatures.

In the Fig. 2.3 one can observe small shift of the maximum of $g(r)$ plot for the first peak at the $T = 240$ K, comparing to the other temperatures. It means that the orientation at the lowest temperature differs from these at the higher. As we pointed earlier, the 5CB molecules tried to penetrate C60 surface at the higher temperatures. The shift is caused by an attempt to penetrate the fullerene wall by mesogen molecules, when they have higher kinetic energy. 5CB molecules are not able to destroy C60 surface because the interaction between fullerenes is strong.

We have also calculated the thermal activation of translational diffusion for the studied system, using the Arrhenius law:

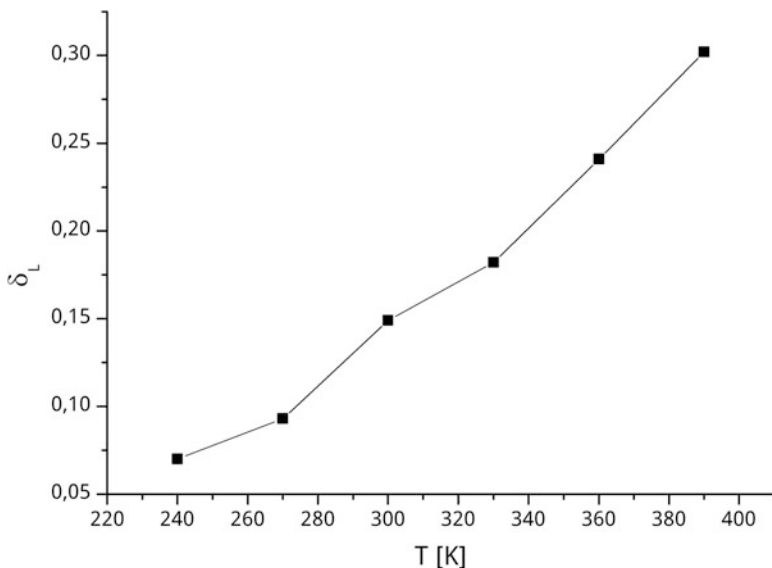


Fig. 2.4 The evolution of Lindemann index obtained for 5CB molecules

$$D = D_0 \exp\left(\frac{E_A}{k_B T}\right),$$

where k_B is the Boltzmann constant and E_A is the activation energy. Fitting data with the Arrhenius law allowed us to estimate the diffusion activation energy E_A , which is equal to 1799 K.

Figure 2.5 shows the values of the second-rank order parameter P_2 , averaged over all time steps. The values of P_2 parameter diminish almost linearly with the heating of the cluster up to the temperature equal to 330 K. For the higher temperatures, the declines of the value of P_2 are practically unnoticeable.

2.4 Conclusions

5CB molecules tried to penetrate C60 surface by immersing themselves between fullerene molecules. This process proceeds with the heating of the system.

At the lowest temperature studied, the mesogen molecules are in the solid state. We have found that the phase transition occurs between $T = 270$ and 300 K.

The orientation of 5CB molecules differs in various temperatures. It is caused by an attempt to penetrate fullerene surface by liquid crystal molecules.

The behavior of 5CB molecules on the C60 surface was examined because it can be interesting for potential applications, for example, in nanotechnology.

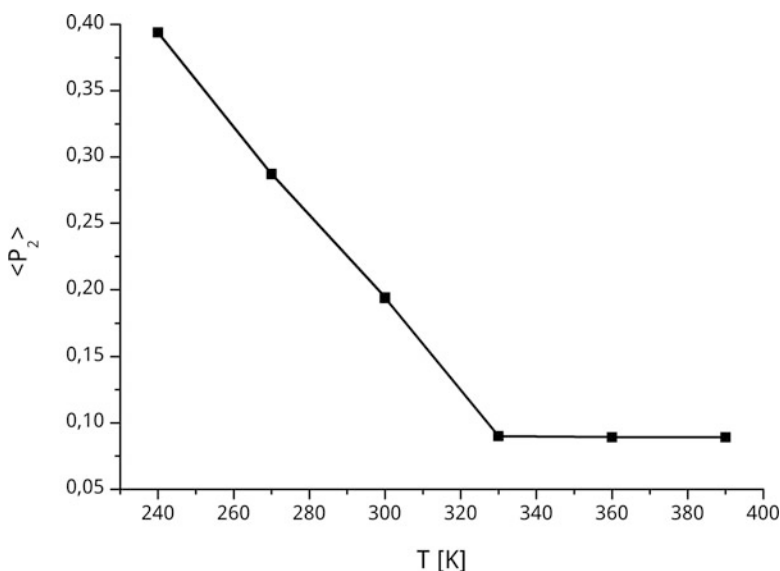


Fig. 2.5 The evolution of second rank order parameter obtained over all time steps, for 5CB molecules

References

1. Yan XQ, Lu YJ (2015) Mechanism of abnormally slow crystal growth of CuZr alloy. *J Chem Phys* 143:164503. doi:[10.1063/1.4934227](https://doi.org/10.1063/1.4934227)
2. Ewiss MAZ, Moawia F, Stoll B (2007) Molecular alignment of the 4-octyl-4'-cyanobiphenyl liquid crystal filled with SiO₂. *Liq Cryst* 34:127–133. doi:[10.1080/02678290601076213](https://doi.org/10.1080/02678290601076213)
3. Gwizdala W, Gorny K, Gburski Z (2008) Molecular dynamics and dielectric loss in 4-cyano-4-n-pentylbiphenyl (5CB) mesogene film surrounding carbon nanotube—computer simulation. *J Mol Struct* 887:148–151. doi:[10.1016/j.molstruc.2007.12.045](https://doi.org/10.1016/j.molstruc.2007.12.045)
4. Bag S, Maingi V, Maiti PK, Yelk J, Glaser MA, Walba DM, Clark NA (2015) Molecular structure of the discotic liquid crystalline phase of hexa-peri-hexabenzocoronene/oligothiophene hybrid and their charge transport properties. *J Chem Phys* 143:144505. doi:[10.1063/1.4932373](https://doi.org/10.1063/1.4932373)
5. Gwizdala W, Gorny K, Gburski Z (2011) The dynamics of 4-cyano-4-n-pentylbiphenyl (5CB) mesogen molecules located between graphene layers-MD study. *Spectrochim Acta Mol Biomol Spectrosc* 79:701–704. doi:[10.1016/j.saa.2010.08.040](https://doi.org/10.1016/j.saa.2010.08.040)
6. Shahinyan AA, Hakobyan PK, Arsenyan LH, Poghosyan AH (2012) The study of lyotropic liquid crystal structure using the molecular dynamics simulation method. *Mol Cryst Liq Cryst* 561:155–169. doi:[10.1080/15421406.2012.687174](https://doi.org/10.1080/15421406.2012.687174)
7. Gorny K, Raczynski P, Dendzik Z, Gburski Z (2015) Odd-even effects in the dynamics of liquid crystalline thin films on the surface of single walled carbon and silicon carbide nanotubes: computer simulation study. *J Phys Chem C* 119:19266–19271. doi:[10.1021/acs.jpcc.5b05961](https://doi.org/10.1021/acs.jpcc.5b05961)
8. Stieger T, Schoen M, Mazza MG (2014) Effects of flow on topological defects in a nematic liquid crystal near a colloid. *J Chem Phys* 140:054905. doi:[10.1063/1.4862953](https://doi.org/10.1063/1.4862953)

9. Iijima S (1991) Helical microtubules of graphitic carbon. *Nature* 354:56–58. doi:[10.1038/354056a0](https://doi.org/10.1038/354056a0)
10. Skrzypek A, Dendzik Z, Brol P, Gburski Z (2004) Cluster and layers of fullerene molecules between graphite planes. *J Mol Struct* 704:287–290. doi:[10.1016/j.molstruc.2004.02.045](https://doi.org/10.1016/j.molstruc.2004.02.045)
11. Tong L, Liu Y, Dolash BD, Jung Y, Slipchenko MN, Bergstrom DE, Cheng J-X (2012) Label-free imaging of semiconducting and metallic carbon nanotubes in cells and mice using transient absorption microscopy. *Nat Nanotechnol* 7:56–61. doi:[10.1038/nnano.2011.210](https://doi.org/10.1038/nnano.2011.210)
12. Keren S, Zavaleta C, Cheng Z, de la Zerda A, Gheysens O, Gambhir SS (2008) Noninvasive molecular imaging of small living subjects using Raman spectroscopy. *Proc Natl Acad Sci* 105:5844–5849. doi:[10.1073/pnas.0710575105](https://doi.org/10.1073/pnas.0710575105)
13. Dawid A, Gburski Z (2003) Rayleigh light scattering in fullerene covered by a spherical argon film—a molecular dynamics study. *J Phys: Condens Matter* 15:2399–2405. doi:[10.1088/0953-8984/15/14/315](https://doi.org/10.1088/0953-8984/15/14/315)
14. Welsher K, Sherlock SP, Dai H (2011) Deep-tissue anatomical imaging of mice using carbon nanotube fluorophores in the second near-infrared window. *Proc Natl Acad Sci* 108:8943–8948. doi:[10.1073/pnas.1014501108](https://doi.org/10.1073/pnas.1014501108)
15. Delogu LG, Vidili G, Venturelli E, Ménard-Moyon C, Zoroddu MA, Pilo G, Nicolussi P, Ligios C, Bedognetti D, Sgarrella F, Manetti R, Bianco A (2012) Functionalized multiwalled carbon nanotubes as ultrasound contrast agents. *Proc Natl Acad Sci* 109:16612–16617. doi:[10.1073/pnas.1208312109](https://doi.org/10.1073/pnas.1208312109)
16. Raczynski P, Dawid A, Gburski Z (2005) Depolarized light scattering in small fullerene clusters—computer simulation. *J Mol Struct* 744:525–528. doi:[10.1016/j.molstruc.2004.12.064](https://doi.org/10.1016/j.molstruc.2004.12.064)
17. Ali-Boucetta H, Kostarelos K (2013) Carbon nanotubes in medicine & biology—therapy and diagnostics. *Adv Drug Deliv Rev* 65:1897–1898. doi:[10.1016/j.addr.2013.11.002](https://doi.org/10.1016/j.addr.2013.11.002)
18. Phillips JC, Braun R, Wang W, Gumbart J, Tajkhorshid E, Villa E, Chipot C, Skeel RD, Kalé L, Schulten K (2005) Scalable molecular dynamics with NAMD. *J Comput Chem* 26:1781–1802. doi:[10.1002/jcc.20289](https://doi.org/10.1002/jcc.20289)
19. Humphrey W, Dalke A, Schulten K (1996) VMD—visual molecular dynamics. *J Mol Graph* 14:33–38
20. Tiberio G, Muccioli L, Berardi R, Zannoni C (2009) Towards in silico liquid crystals realistic transition temperatures and physical properties for n-cyanobiphenyls via molecular dynamics simulations. *ChemPhysChem* 10:125–136. doi:[10.1002/cphc.200800231](https://doi.org/10.1002/cphc.200800231)
21. Hilder TA, Pace RJ, Chung S-H (2012) Computational design of a carbon nanotube fluorofullerene biosensor. *Sensors* 12:13720–13735. doi:[10.3390/s121013720](https://doi.org/10.3390/s121013720)
22. D’Avino G, Muccioli L, Zannoni C (2015) From chiral islands to smectic layers: a computational journey across sexithiophene morphologies on C60. *Adv Funct Mater* 25:1985–1995. doi:[10.1002/adfm.201402609](https://doi.org/10.1002/adfm.201402609)

Nanophysics, Nanophotonics, Surface Studies, and
Applications

Selected Proceedings of the 3rd International
Conference Nanotechnology and Nanomaterials
(NANO2015), August 26-30, 2015, Lviv, Ukraine

Fesenko, O.; Yatsenko, L. (Eds.)

2016, XXV, 593 p. 316 illus., 151 illus. in color.,

Hardcover

ISBN: 978-3-319-30736-7